

IMPACT OF FOREGROUNDS ON COSMIC MICROWAVE BACKGROUND MAPS

G. DE ZOTTI

INAF-Osservatorio Astronomico di Padova, Vicolo Osservatorio 5, I-35122 Padova, Italy
E-mail: dezotti@pd.astro.it

C. BURIGANA

IASF/CNR, Sezione di Bologna, Via Gobetti 101, I-40129 Bologna, Italy
E-mail: burigana@bo.iasf.cnr.it

C. BACCIGALUPI AND R. RICCI

SISSA, Via Beirut 4, I-34014 Trieste, Italy
E-mail: bacci,ricci@sissa.it

We discuss the possible impact of astrophysical foregrounds on three recent exciting results of Cosmic Microwave Background (CMB) experiments: the WMAP measurements of the temperature-polarization (*TE*) correlation power spectrum, the detection of CMB polarization fluctuations on degree scales by the DASI experiment, and the excess power on arcminute scales reported by the CBI and BIMA groups. A big contribution from the Galactic synchrotron emission to the *TE* power spectrum on large angular scales is indeed expected, in the lower frequency WMAP channels, based on current, albeit very uncertain, models; at higher frequencies the rapid decrease of the synchrotron signal may be, to some extent, compensated by polarized dust emission. Recent measurements of polarization properties of extragalactic radio sources at high radio frequency indicate that their contamination of the CMB polarization on degree scales at 30 GHz is substantially below the expected CMB *E*-mode amplitude. Adding the synchrotron contribution, we estimate that the overall foreground contamination of the signal detected by DASI may be significant but not dominant. The excess power on arc-min scales detected by the BIMA experiment may be due to galactic-scale Sunyaev-Zeldovich effects, if the proto-galactic gas is heated to its virial temperature and its cooling time is comparable to the Hubble time at the epoch of galaxy formation. A substantial contamination by radio sources of the signal reported by the CBI group on scales somewhat larger than BIMA's cannot be easily ruled out.

1. Introduction

For a lucky, at least from the cosmologist's point of view, coincidence, the spectral energy distribution of most classes of extragalactic sources has a minimum at millimeter wavelengths, fortuitously close to the peak of the Cosmic Microwave Background (CMB) spectrum. At high Galactic latitudes the minimum is a factor of few $\times 10^{-6}$ below the peak CMB intensity; correspondingly, foreground fluctuations

can be below the μK level, allowing a clean detection of CMB anisotropies.

This “cosmological window”, extending roughly over the frequency range 40–150 GHz, is crucial to exploit in depth the extraordinary information content of the CMB: in fact, with current technologies the limit is not set by instrumental sensitivity but by the contamination by astrophysical foregrounds.

The situation is actually slightly different when we are dealing with CMB anisotropies rather than with total intensity. On angular scales larger than $\simeq 30'$ foreground fluctuations are essentially of Galactic origin and are minimum around 60 GHz⁵. On smaller scales, extragalactic sources take over, and the minimum shifts to 100–150 GHz.

The minimum in the spectrum arises from a superposition of two emission mechanisms. The radio emission is generally – but not always – dominated by optically thin synchrotron, which decreases with frequency with a power law spectrum (flux density $\propto \nu^\alpha$, with $\alpha \sim -0.5$ to -1.0). At wavelengths shorter than a few mm, again for typical sources, the emission is dominated by thermal dust, whose spectrum increases sharply with frequency ($\alpha \simeq 4$). Just because of such steep rise, the frequency of the minimum is only weakly dependent on the relative intensity of the two components. Moreover, the effect of redshift on the dust emission peak is to some extent compensated by the dust temperature increase associated with the luminosity evolution of sources. Thus the smearing effect of the variance in the source properties and of the redshift distribution is limited and the minimum is quite deep.

Nevertheless, distinguishing the cosmological signal from foreground contamination is one of the main challenges facing the most sensitive CMB experiments. We will illustrate this issue with reference to three recent exciting results: i) WMAP measurements of the temperature-polarization correlation power spectrum^{4,25}; ii) the detection of degree-scale polarization fluctuations by the DASI experiment²⁷; iii) the excess power on arcminute scales detected by the CBI^{30,35} and BIMA¹² experiments.

2. WMAP measurements of temperature-polarization correlation

Primordial adiabatic density fluctuations create, at decoupling, polarization either perpendicular or parallel to the wave vector, i.e. a curl-free pattern referred to as *E*-mode polarization^{23,52}. Since *E*-mode polarization is related to peculiar velocities on the last scattering surface, the peaks of its power spectrum are tightly related with those of temperature anisotropies, being out of phase by $\pi/2$ since velocities are out of phase with density perturbations like velocity and position of a harmonic oscillator: velocities drop to zero at the compression or rarefaction maxima.

Given such tight correlation and the low level of CMB polarization, compared to temperature (*T*) anisotropies, it is easily understood that the *TE* correlation has the largest amplitude among CMB power spectra involving polarization. Its detection is further eased by the fact that this is not true, in general, for fore-

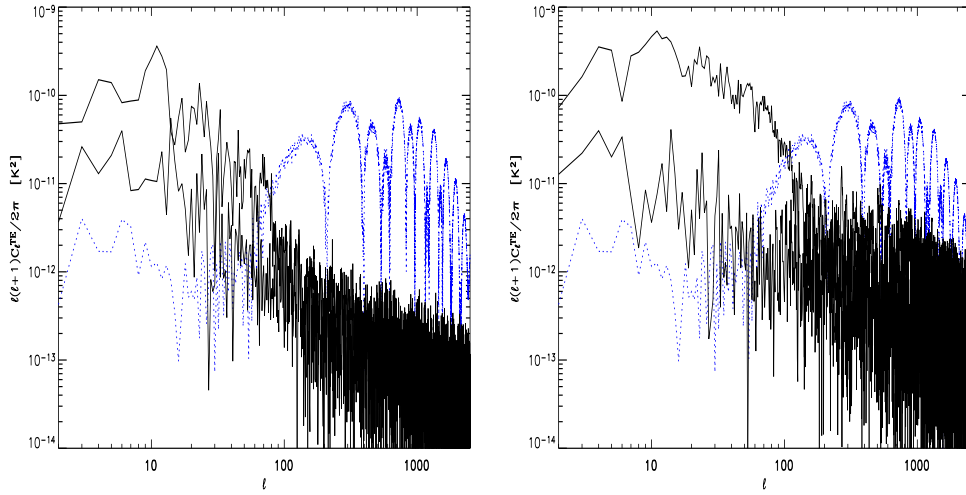


Figure 1. Power spectrum of the TE correlation for Galactic synchrotron emission predicted by the models by² (left panel) and¹⁸ (right), extrapolated assuming that its antenna temperature has a spectral index of -2.9 ($T_{\text{ant}} \propto \nu^{-2.9}$). The upper curve shows an all-sky average, the lower one refers to high Galactic latitudes ($|b| > 20^\circ$) only. Also shown is the CMB TE spectrum (curve with multiple peaks, dominating at high multipoles) based on a simulation using the best fit values of the cosmological parameters obtained by⁴⁰ (last column of their Table 7) taking into account also large scale structure data, plus a tensor component with a ratio of tensor to scalar contributions to the temperature quadrupole $T/S = 0.3$. The re-ionization optical depth is $\tau = 0.117$.

grounds. In the limiting case of a random distribution of polarization angles, as in the case of uncorrelated point sources, the power spectrum of the correlation of T with the Stokes parameters Q and U , characterizing linear polarization, vanishes: $\langle T\{Q, U\} \rangle_{\text{foreground}} = \langle T^2 p \cos(2\phi) \rangle = 0$, where p is the polarization degree.

But in the case of Galactic synchrotron emission, the orderly large scale magnetic field may translate in a $TE_{\text{Gal.synch}}$ comparable to, or larger than TE_{CMB} . This is illustrated by Fig. 1 where the power spectra at 30 GHz of the $TE_{\text{Gal.synch}}$ correlation predicted by two recent models^{2,18} are compared with TE_{CMB} . The $TE_{\text{Gal.synch}}$ power spectrum was computed in two cases: either as an average over the full sky or restricting ourselves to high-galactic latitudes ($|b| > 20^\circ$). $TE_{\text{Gal.synch}}$ drops on small angular scales (large multipoles ℓ) due to the effect of the chaotic component of the magnetic field. On the other hand, both models predict, on large scales, a $TE_{\text{Gal.synch}}$ power spectrum exceeding that due to the CMB. Clearly, both models are highly uncertain due to our poor knowledge of the Galactic polarized emission, and the WMAP data already indicate that they grossly overestimate $TE_{\text{Gal.synch}}$. However, a significant Galactic contribution to the TE signal measured by WMAP at the lowest frequencies cannot be ruled out easily.

Figure 2 shows that the synchrotron signal drops dramatically (compared to the

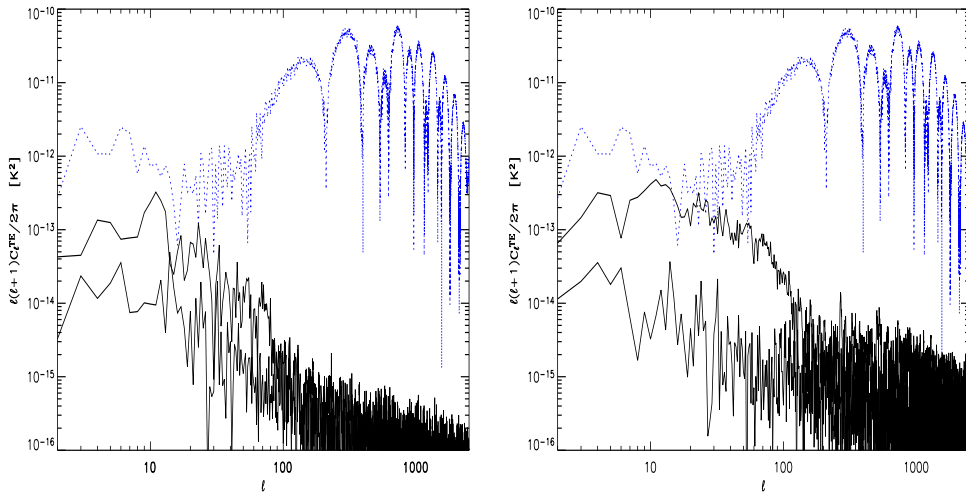


Figure 2. Same as in Fig. 1, but a 100 GHz.

CMB signal) at high frequencies. This steep frequency dependence backs up the conclusion that the TE signal detected by WMAP, which is consistent with being frequency-independent^{4,25}, is not seriously affected by Galactic contamination. Some caution, however, may still be necessary in interpreting these data. In fact, the recent ARCHEOPS experiment has detected⁶ large scale polarized emission (polarization degree at the 4–5% level) from Galactic dust grains aligned by a coherent magnetic field coplanar to the Galactic plane. Such emission, steeply rising with frequency, is associated to the same magnetic field responsible for synchrotron emission, and may to some extent compensate for the drop of the synchrotron component at high frequencies.

3. CMB polarization fluctuations on degree scales

The first direct detection of CMB E -mode polarization may have been achieved by the DASI experiment²⁷, at 30 GHz, on degree scales. The most significant detection was achieved at $\ell \sim 300$, which, at the frequency of observations, roughly corresponds to the transition between the large scales where the foreground power spectrum is expected to be dominated by Galactic synchrotron and the smaller scales where the most important contamination comes from polarized emission from extragalactic radio sources.

The observational information on polarized synchrotron emission is limited to low frequencies, which may be affected by Faraday depolarization. On degree and sub-degree angular scales only a few patches of the sky, mostly at low Galactic latitude have been observed^{16,17,49,50,44}. In particular, there are no published polarization maps in the region observed by the DASI experiment²⁷.

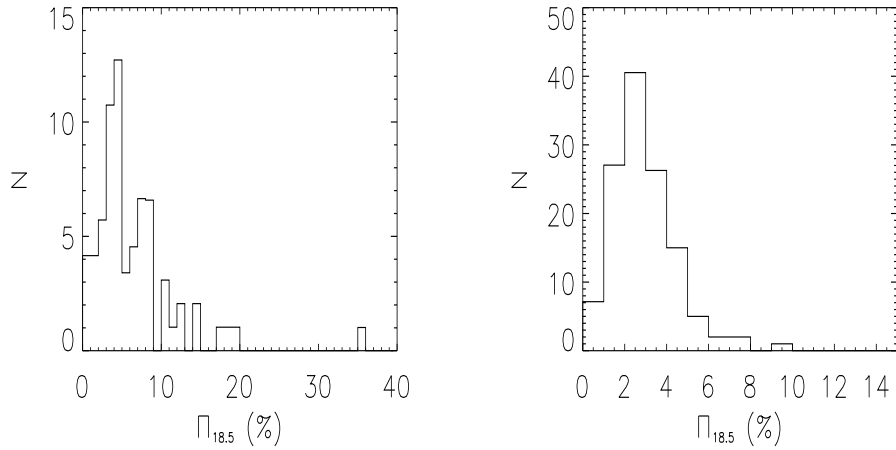


Figure 3. Distribution of the fractional polarization degree at 18.5 GHz of Southern Kühr steep-spectrum (left) and flat-spectrum (right) sources³⁸.

Since the polarized Galactic synchrotron emission varies substantially across the sky, any estimate is highly uncertain. However, the estimates based on the available information^{46,47,2,3,11,10,13} do suggest that the synchrotron contamination is likely to be below the signal detected by the DASI experiment, consistent with the discussion in²⁷.

Estimates of polarization fluctuations due to extragalactic radio sources are also affected by considerable uncertainty^{39,14,31,48}. Again, the dominant emission process is synchrotron, whose radiation is intrinsically highly polarized. Yet the observed polarization degree of most sources observed at MHz or GHz frequencies is not higher than a few percent. Possible explanations may be a strong Faraday depolarization or highly turbulent magnetic fields. Thus, a strong frequency dependence of the polarization degree may be expected. Measurements at high frequencies are necessary!

A good opportunity in this direction is offered by the major millimeter up-grade of the Australia Telescope Compact Array (ATCA), which is going on since 2001. In the commissioning phase, the prototype receivers mounted on three antennas were used³⁸ to take snapshots at 18.5 GHz of 250 out of the 258 Southern extragalactic sources in the complete 5 GHz 1 Jy sample²⁸. The configuration is very compact, yielding a beam-width of $15.6''$ at the observing frequency. Due to poor phase calibration, flux densities could only be reliably determined for sources that can be successfully fitted by the point-source model. This resulted in the rejection of 53 sources.

The majority of rejected sources (40 out of 53) are steep-spectrum, consistent

with the fact that steep-spectrum sources are frequently extended. Also, these sources are obviously fainter at high frequencies so that their polarization is more difficult to measure. On the whole, polarization measurements were obtained for only $\simeq 50\%$ of observed steep-spectrum sources, and upper limits were determined for an additional 13%. Thus, the results for these sources are somewhat uncertain and affected by a bias against extended sources. However, these uncertainties are not critical for the estimate of polarization fluctuations at the frequencies of CMB experiments, since in any case, flat-spectrum sources dominate there.

The distribution of polarization degrees of steep-spectrum sources at 18.5 GHz, $\Pi_{18.5}$, obtained using the Kaplan-Meier estimator to take into account also upper limits, is shown in the left-hand panel of Fig. 3. The median value is $\Pi_{18.5} \simeq 4.8\%$, and the mean is $6.5 \pm 0.7\%$. The 37 steep-spectrum sources in common with the NVSS survey have a median polarization degree at 1.4 GHz of only $\simeq 0.4\%$; there is thus clear evidence of a strong frequency dependence of the polarization degree for these sources.

The polarization degree was measured for 80% of the flat-spectrum sub-sample; including upper limits, we have data for 88% of these sources. The distribution of their polarization degrees, obtained again with the Kaplan-Meier estimator, is shown in the right-hand panel of Fig. 3. Allowing for upper limits, the median value is found to be $\Pi_{18.5} \simeq 2.7\%$, the mean $2.9 \pm 0.1\%$. The median polarization degree at 1.4 GHz of sources in common with the NVSS survey is 1.4%. Thus, there is a much weaker frequency dependence of the polarization degree than in the case of steep-spectrum sources. A closer look at the distribution of $\Pi_{18.5}$ against $\Pi_{1.4}$ shows that sources with $\Pi_{1.4}$ larger than $\simeq 2\%$ have, on average, a similar polarization degree both at low and high frequency, while sources with lower values of $\Pi_{1.4}$ have relatively large $\Pi_{18.5}/\Pi_{1.4}$ ratios.

Armed with these results, we can now estimate the polarization fluctuations due to extragalactic radio sources and combine them with those due to Galactic synchrotron to derive the total amplitude of foreground fluctuations. The results are shown in Fig. 4. Uncertain as they are, these estimates are consistent with a significant, but not dominant, foreground contamination of the DASI results.

4. The excess power on arcminute scales

Evidences of statistically significant detections at 30 GHz of arcminute scale fluctuations well in excess of predictions for primordial anisotropies of the cosmic microwave background (CMB) have recently been obtained by the CBI³⁰ and BIMA¹² experiments. The interpretation of these results is still debated. Extragalactic sources are potentially the dominant contributor to fluctuations on these scales and must be carefully subtracted out. And indeed both groups devoted a considerable effort for this purpose. However, as discussed by¹⁵, a quite substantial residual contribution to the CBI signal is difficult to rule out, while the residual radio source contamination of the BIMA results is likely to be very small.

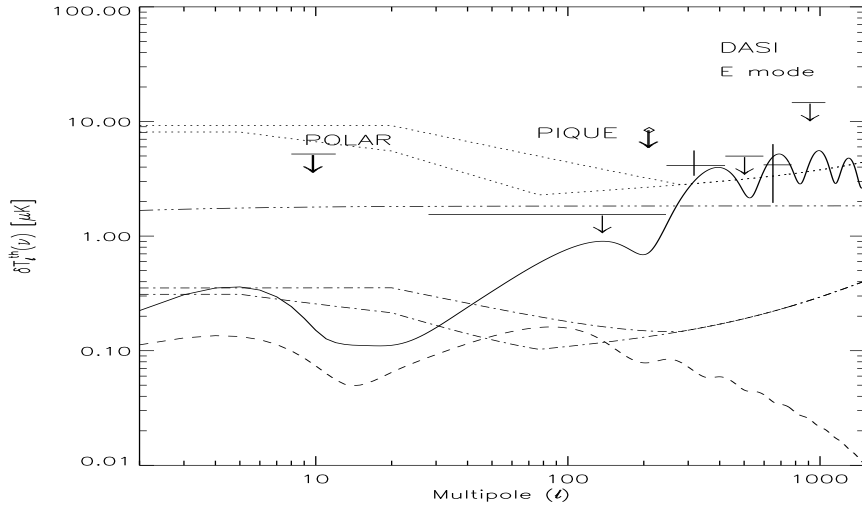


Figure 4. Estimated power spectra of Galactic synchrotron plus point sources at 30 GHz (dotted line) and 100 GHz (dot-dashed line) compared with the CMB *E*-mode (solid line) and *B*-mode (dashed line) power spectra and with the results of the PIQUE²², POLAR³⁴, and DASI²⁷ experiments. The PIQUE experiment operates at 90 GHz, while the POLAR and DASI experiment operate at 30 GHz. The CMB power spectra refer to the same values of the parameters as in Fig. 1. The horizontal line (dash-three dots) shows a tentative estimate of the power spectrum of the polarized emission from Galactic dust at 217 GHz, obtained from the average power spectrum of dust emission at high Galactic latitudes ($|b| \geq 30^\circ$) determined by WMAP⁵, extrapolated to 217 GHz assuming a spectral slope of 2.2 in antenna temperature ($T_{\text{ant}} \propto \nu^{2.2}$), as indicated by WMAP results, and adopting a polarization degree of 5%⁶. The pair of lines at 30 and 100 GHz, for $\ell < 200$, bound the range of synchrotron power spectra found by Burigana & La Porta¹¹, extrapolated to 30 GHz assuming an antenna temperature spectral index of -2.9 . Note that the POLAR upper limit on large angular scales is already below the lowest expectation for the synchrotron signal. This may indicate that the synchrotron spectral index is steeper than assumed (e.g. $\simeq -3.1$) or that the polarized synchrotron emission is below average in area covered by the POLAR experiment. The minimum at $\ell \sim 100-200$ in the foreground power spectra at 30 and 100 GHz correspond to the transition between the angular scales where the dominant polarized emission is synchrotron (lower values of ℓ) to the region where extragalactic radio sources take over.

If indeed the detected signal cannot be attributed to extragalactic radio sources, its most likely source is the thermal Sunyaev-Zeldovich^{41,42,43} (SZ) effect¹⁹. The SZ within rich clusters of galaxies has been extensively investigated^{26,9}. The estimated power spectrum was found to be very sensitive to the normalization (σ_8) of the density perturbation spectrum. A $\sigma_8 \gtrsim 1$, somewhat higher than indicated by other data sets, is apparently required to account for the CBI data.

A preliminary analytical investigation of the SZ signals associated to the formation of spheroidal galaxies has been carried out by¹⁵. They point out that the proto-galactic gas is expected to have a large thermal energy content, leading to a detectable SZ signal, both when the protogalaxy collapses with the gas shock-heated to the virial temperature^{37,51}, and in a later phase as the result of strong

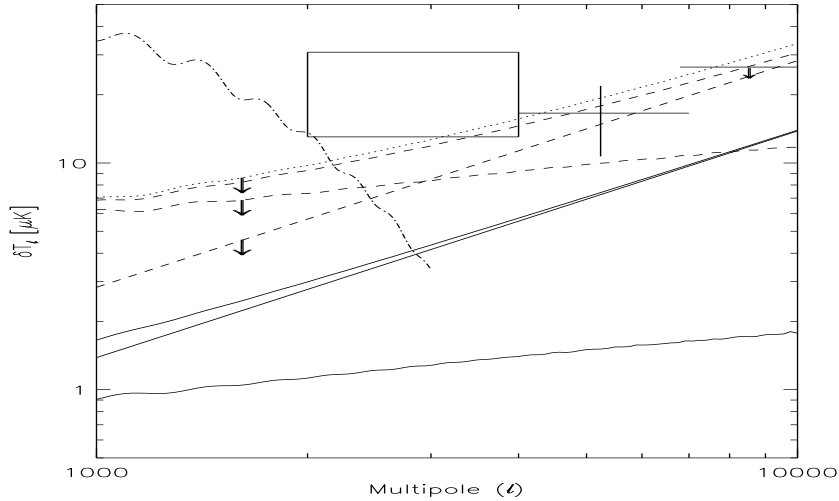


Figure 5. Possible contributions of galaxy-scale Sunyaev-Zeldovich effects to the excess power on sub-arcmin scales detected by the CBI³⁰ (box) and BIMA¹² (cross and upper limit on the upper right corner) experiments. The dot-dashed line shows the CMB power spectrum for the set of cosmological parameters specified in the caption to Fig. 1. The dashed lines refer to the contributions from proto-galactic gas at virial temperature; the line with the steepest slope shows the Poisson contribution, that with the flattest slope shows the contribution due to clustering, while the highest dashed line gives the sum of the two contributions. The downward pointing arrows indicate that the adopted values of the parameters tend to maximize the signal. The solid lines show the contributions due to the heating of the interstellar medium by quasar feedback; again the line with the steepest and with the flattest slope correspond to the Poisson and clustering contributions, respectively, while the upper solid line shows the sum of the two contributions. The dotted line is the sum of all contributions.

feedback from a flaring active nucleus^{24,33,32,1,36,29}.

These SZ signals, showing up on sub-arcmin scales, are potentially able to account for the BIMA results. Proto-galactic gas heated at the virial temperature and with a cooling time comparable with the expansion time may provide the dominant contribution (see Fig. 5); in this case we expect clustering fluctuations of amplitude comparable to Poisson fluctuations, although with a flatter power spectrum. As stressed by¹⁵, the estimate of the signal from the gas at the virial temperature is based on an over-simplified treatment. In fact, the thermal history of the proto-galactic gas is quite complex: only a fraction of it may be heated to the virial temperature^{7,8}; cooling may be relatively rapid in the densest regions while significant heating may be provided by supernovae and by the central active nucleus. On the other hand, the SZ effect turns out to be an effective probe of the thermal state of the gas and of its evolution so that its detection would provide unique information on early phases of galaxy evolution, essentially unaccessible by other means.

The SZ signals produced by strong feedback from the central active nucleus have been discussed in the framework proposed by^{20,21}, whereby the interplay

between star formation and nuclear activity in large spheroidal galaxies is the key to overcome some of the crises of the currently standard scenario for galaxy evolution.

This scenario envisages powerful quasar driven outflows, carrying a considerable fraction of the quasar bolometric luminosity, L_{bol} , increasing as $L_{\text{bol}}^{1/2}$ (for emission close to the Eddington limit). For large enough galaxies ($M_{\text{vir}} \gtrsim 10^{12} M_{\odot}$) these outflows eventually sweep out the interstellar medium (ISM) thus switching off the star-formation on shorter timescales for more massive objects, consistent with their observed α -enhancement⁴⁵. The outflows are expected to be highly supersonic, and therefore liable to induce strong shocks, transiently heating the interstellar gas to temperatures exceeding the virial value by a substantial factor. The associated SZ signals are correspondingly stronger, albeit much rarer, than those due to the proto-galactic gas heated at the virial temperature, discussed above.

A direct detection of individual SZ effects can be achieved by the forthcoming large area high frequency surveys. We expect a surface density of $\simeq 1 \text{ deg}^{-2}$ at $S_{30\text{GHz}} \simeq 1 \text{ mJy}$. Of course, the counts at these relatively bright fluxes are likely dominated by SZ effects in clusters of galaxies, which however should be easily distinguishable because of their much larger angular size and much lower redshift.

Work supported in part by MIUR and ASI.

References

1. N. Aghanim, C. Balland and J. Silk, *A&A*, **357**, 1 (2000).
2. C. Baccigalupi *et al.*, *A&A*, **372**, 8 (2001).
3. C. Baccigalupi, G. De Zotti, C. Burigana and F. Perrotta, in *Astrophysical Polarized Backgrounds*, ed. S. Cecchini, S. Cortiglioni, R. Sault and C. Sbarra, AIP Conf. Proc. **609**, 84 (2002).
4. C.L. Bennett *et al.*, *ApJS*, **148**, 1 (2003).
5. C.L. Bennett *et al.*, *ApJS*, **148**, 97 (2003).
6. A. Benoit *et al.*, *A&A*, submitted, astro-ph/0306222 (2003).
7. J. Binney, *MNRAS*, submitted, astro-ph/0308172 (2003).
8. Y. Birnboim and A. Dekel A., *MNRAS*, **345**, 349 (2003).
9. J.R. Bond *et al.*, *ApJ*, submitted, astro-ph/0205386 (2003).
10. M. Bruscoli, M. Tucci, V. Natale, E. Carretti, R. Fabbri, C. Sbarra and S. Cortiglioni, *NewA*, **7**, 171 (2002).
11. C. Burigana and L. La Porta, in *Astrophysical Polarized Backgrounds*, ed. S. Cecchini, S. Cortiglioni, R. Sault and C. Sbarra, AIP Conf. Proc. **609**, 54 (2002).
12. K.S. Dawson, W.L. Holzapfel, J.E. Carlstrom, M. Joy, S.J. LaRoque, A.D. Miller and D. Nagai, *ApJ*, **581**, 86 (2002).
13. G. De Zotti, in *Astrophysical Polarized Backgrounds*, ed. S. Cecchini, S. Cortiglioni, R. Sault and C. Sbarra, AIP Conf. Proc. **609**, 295 (2002).
14. G. De Zotti, C. Gruppioni, P. Ciliegi, C. Burigana and L. Danese, *NewA*, **4**, 481 (1999).
15. G. De Zotti, C. Burigana, A. Cavaliere, L. Danese, G.L. Granato, A. Lapi, P. Platania and L. Silva, in *Plasmas in the Laboratory and in the Universe: new insights and new challenges*, in press (2003).
16. A.R. Duncan, R.F. Haynes, K.L. Jones and R.T. Stewart, *MNRAS*, **291**, 279 (1997).
17. A.R. Duncan, P. Reich, W. Reich and E. Fürst, *A&A*, **350**, 447 (1999).

18. G. Giardino, A.J. Banday, K.M. Górski, K. Bennett, J.L. Jonas and J. Tauber, *A&A*, **387**, 82 (2002).
19. N.Y. Gnedin and A.H. Jaffe, *ApJ*, **551**, 3 (2001).
20. G.L. Granato, L. Silva, P. Monaco, P. Panuzzo, P. Salucci, G. De Zotti and L. Danese, *MNRAS*, **324**, 757 (2001).
21. G.L. Granato, G. De Zotti, L. Silva, A. Bressan and L. Danese, *ApJ*, submitted, astro-ph/0307202 (2003).
22. M.M. Hedman, D. Barkats, J.O. Gundersen, J.J. McMahon, S.T. Staggs and B. Winstein, *ApJ*, **573**, L73 (2002).
23. W. Hu and M. White, *NewA*, **2**, 323 (1997).
24. S. Ikeuchi, *PASJ*, **33**, 211 (1981).
25. A. Kogut *et al.*, *ApJS*, **148**, 161 (2003).
26. E. Komatsu and T. Kitayama, *ApJ*, **526**, L1 (1999).
27. J.M. Kovac, E.M. Leitch, C. Pryke, J.E. Carlstrom, N.W. Halverson and W.L. Holzapfel, *Nature*, **420**, 772 (2002).
28. H. Kühr, A. Witzel, I.I.K. Pauliny-Toth and U. Nauber, *A&AS*, **45**, 367 (1981).
29. A. Lapi, A. Cavaliere and G. De Zotti, *ApJ*, **597**, L93 (2003).
30. B.S. Mason *et al.*, *ApJ*, **591**, 540 (2003).
31. D. Mesa, C. Baccigalupi, G. De Zotti, L. Gregorini, K.-H. Mack, M. Vigotti and U. Klein, *A&A*, **396**, 463 (2002).
32. P. Natarajan and S. Sigurdsson, *MNRAS*, **302**, 288 (1999).
33. P. Natarajan, S. Sigurdsson and J. Silk, *MNRAS*, **298**, 577 (1998).
34. C.W. O'Dell, B.G. Keating, A. de Oliveira-Costa, M. Tegmark and P.T. Timbie, *Phys. Rev. D*, **68**, 42002 (2003).
35. T.J. Pearson *et al.*, *ApJ*, **591**, 556 (2003).
36. P. Platania, C. Burigana, G. De Zotti, E. Lazzaro and M. Bersanelli, *MNRAS*, **337**, 242 (2002).
37. M.J. Rees and J.P. Ostriker, *MNRAS*, **179**, 541 (1977).
38. R. Ricci, C. Gruppioni, I. Prandoni, R.J. Sault and G. De Zotti, *A&A*, in press (2003).
39. M.V. Sazhin and V.A. Korolëv, *Pis'ma Astr. Zh.*, **11**, 490, engl. transl. *Sov. Astr. Lett.*, **11**, 204 (1985).
40. D.N. Spergel *et al.*, *ApJS*, **148**, 175 (2003).
41. R.A. Sunyaev and Ya.B. Zeldovich, *Com. Ap.*, **4**, 173 (1972).
42. R.A. Sunyaev and Ya.B. Zeldovich, *ARA&A*, **18**, 537 (1980).
43. R.A. Sunyaev and Ya.B. Zeldovich, *SSRvE*, **1**, 1 (1981).
44. A.R. Taylor *et al.*, *AJ*, **125**, 3145 (2003).
45. D. Thomas, C. Maraston and R. Bender, *Rev. Mod. Astr.*, **15**, 219 (2002).
46. M. Tucci, E. Carretti, S. Cecchini, R. Fabbri, M. Orsini, E. Pierpaoli, *NewA*, **5**, 181 (2000).
47. M. Tucci *et al.*, *ApJ*, **579**, 607 (2002).
48. M. Tucci, E. Martínez-González, L. Toffolatti, J. González-Nuevo and G. De Zotti, *MNRAS*, submitted, astro-ph/0307073 (2003).
49. B. Uyaniker, E. Fürst, W. Reich, P. Reich and R. Wielebinski R., *A&AS*, **132**, 401 (1998).
50. B. Uyaniker, T.L. Landecker, A.D. Gray and R. Kothes, *ApJ*, **585**, 785 (2003).
51. S.D.M. White and M.J. Rees, *MNRAS*, **183**, 341 (1978).
52. M. Zaldarriaga and U. Seljak, *Phys. Rev. D* **55**, 1930 (1997).